Biomaterials 32 (2011) 1923–1931

Contents lists available at ScienceDirect

Biomaterials

journal homepage: www.elsevier.com/locate/biomaterials

Quantum dot-antisense oligonucleotide conjugates for multifunctional gene transfection, mRNA regulation, and tracking of biological processes

Yilin Li, Xin Duan, Lihong Jing, Chunhui Yang, Ruirui Qiao, Mingyuan Gao*

Institute of Chemistry, The Chinese Academy of Sciences, Bei Yi Jie 2, Zhong Guan Cun, 100190 Beijing, China

ARTICLE INFO

Article history:
Received 31 October 2010
Accepted 14 November 2010
Available online 9 December 2010

Keywords:
CdTe QDs
Antisense oligonucleotides
Gene transfection
Intracellular localization
Apoptosis

ABSTRACT

It was demonstrated that oligonucleotides, independent of their base sequence and length, could effectively induce the cellular uptake of mercapto acid-capped CdTe QDs after the oligonucleotides were covalently attached on the surface of the QDs. Following these experimental observations, a conjugate composed of covalently linked anti-survivin antisense oligonucleotides (ASON) and CdTe QDs was designed and synthesized. Then, the survivin mRNA down-regulation and the apoptosis of HeLa cells induced by ASON were studied. Systematic experimental results revealed that CdTe-ASON could effectively induce the apoptosis of HeLa cells, while CdTe QDs offered the possibility to visualize the specific intracellular localization of the CdTe-ASON probes strongly associated with their biological functions.

1. Introduction

Quantum dots (QDs) are now considered as a new class of fluorescent probes both in biology and in biomedicine [1–10]. As the fluorescence of QDs - in comparison with that of conventional dyes - is characterized by narrow, symmetric, and particle size-dependent features, as well as a broad excitation range and excellent robustness against photobleaching, they are greatly desirable for multiplex immunoassays [4–8], cellular fluorescence imaging [2,3,5,6], and in vivo fluorescence imaging [5,9]. Recently they have also been found to be potentially useful in visually tracking biomolecules inside living cells to elucidate some biological processes at the cellular level [10].

QDs have even been used in recent gene studies [11–21]. For example, in one of the earlier investigations, QDs were used to detect a gene silencing effect after being co-transfected with small interfering RNA (siRNA) using cationic liposomes, upon an assumption that the fluorescence intensity of QDs loaded by cells is directly correlated with the biological effects of siRNA [11]. By attaching plasmid DNA on QDs via a specific interaction between PNA (peptide nucleic acids) on QDs and plasmid DNA, Burgess and co-workers [12] developed a fluorescent probe for intracellular tracking of the plasmid DNA after the probe was delivered using cationic liposomes. Enlightened by the success of using cationic liposomes in gene delivery, various types of cationic lipids [22,23], polymers such as chitosan [14,24], amphipol [16], polyethylenimine [20,25–28], polyphosphoramidate [21], dendrimers [29] and peptides [19,20] were further employed to modify the inorganic nanoparticles so as to enable them as gene vectors. Such cationic surface modification for nanomaterials greatly facilitates both the loading of genes by forming electrostatic complexes and the subsequent release of genes within the cytoplasm, apart from increasing the stability of genes against nuclease degradation [16,30]. Thus, QD-based gene vectors realized by cationic surface modification were successfully developed for monitoring the cellular uptake of foreign genes.

The cellular uptake is undoubtedly one of the most important steps for gene transfection. However, the following endosomal escape, cytoplasmic mobility, and nuclear entry of foreign genes are also very important for in vitro gene transfection with respect to nonviral gene transfection systems [31]. Therefore, to visually track and identify the intracellular localization of a foreign gene would be greatly helpful for revealing the intracellular target sites of the transfected genes, elucidating the biological actions and processes exerted or caused by the transfected genes, and thereby probing the mechanisms of the transfected genes at the cellular level.

To visually track the intracellular behavior of the foreign genes, we prepared a covalent conjugate of anti-survivin antisense oligonucleotide (ASON) and CdTe QDs stabilized by thioglycolic acid (TGA) via an amide bond, based on the experimental observation that oligonucleotides covalently conjugated to CdTe QDs could effectively induce the cellular uptake of the resultant CdTe-oligonucleotide

* Corresponding author. Tel./fax: +86 10 82613214.
E-mail address: gaomy@iccas.ac.cn (M. Gao).

0142-9612/$ – see front matter © 2010 Elsevier Ltd. All rights reserved.
doi:10.1016/j.biomaterials.2010.11.024

conjugates. The use of covalent bonds for constructing the transfection system was expected to be helpful for visually tracking the anti-survivin ASON within cells. Survivin is a member of the inhibitor of apoptosis family of proteins, which can inhibit apoptosis, enhance cell proliferation, and promote angiogenesis. Although it is up-regulated in most cancers, survivin is rarely expressed in normal differentiated tissues, which thus endows survivin with potentials as target for anti-cancer gene therapy [32]. Anti-survivin ASON is a 20-mer single-stranded DNA molecule. Once internalized into cells, anti-survivin ASON is able to complementarily combine with survivin mRNA, and inhibit its expression and ultimately induce the apoptosis of tumor cells [33]. To suppress the influences of CdTe QDs on the biological functions of ASON, an A_9 tether pre-modified at the 5′ end of the ASON was used as a linker between CdTe QDs and ASON, ending up with a 29-mer oligonucleotide (ASON29). In a similar way, conjugates of CdTe QDs and various non-complementary oligonucleotides to survivin mRNA were also synthesized and used as control probes. Then, the endocytic mechanism for CdTe-oligonucleotide probes was investigated by employing various types of endocytosis inhibition reagents. Moreover, the intracellular localization of CdTe-ASON29 was visually tracked by confocal fluorescence microscope. Additionally, the effects of the CdTe-ASON29 conjugates on the down-regulation of survivin mRNA and the apoptosis of HeLa cells were investigated so as to correlate the intracellular localization of CdTe-ASON29 with the biological functions of ASON.

2. Experimental section

2.1. Chemicals

1-ethyl-3-(3-dimethylaminopropyl) carbodiimide (EDC) (97.0%+, product 39391), *N*-hydroxysulfosuccinimide sodium salt (sulfo-NHS) (98.5%+, product 56485) and chlorpromazine hydrochloride (98%+, product C8138) were all purchased from Sigma–Aldrich. Agarose (Biowest Agarose, product 101710) was purchased from Gene Tech. Co., Ltd., Shanghai, China. Tris(hydroxymethyl) aminomethane (Tris) (Amresco, 99.9%, code 0497), 3-(4,5-dimethylthiazol-2-yl)-2,5-diphenyl-2H-tetrazolium bromide (MTT) (Amresco, 98%+, code 0793), dimethyl sulfoxide (DMSO) (Amresco, code 0231) and trypsin (Amresco 1:250, code 0458) were distributed by Biodee Biotechnology Co., Ltd., Beijing, China. Eagle's minimum essential medium (EMEM) (cat. no. 41500-034), TRIzol reagent (cat. no. 15596-026), M-MLV reverse transcriptase (200 U/μl, cat. no. S28025-011), 5-(N-ethyl-N-isopropyl)amiloride hydrochloride (cat.no. E–3111) and cytochalasin D (cyto D) (cat.no. PHZ1063) were purchased from Invitrogen. Methyl-β-cyclodextrin (MβCD) (98%, product 1090769) and genistein (98%+, product 1109860) were purchased from Aladdin Reagent Database Inc., Shanghai, China. Fetal bovine serum (FBS) (part SH3007003) was purchased from Thermo Fisher Scientific Inc. dNTP mixture (10 mM each, code D4030RA), oligo $d(T)_{18}$ primers (14 nmol, code D511), cloned ribonuclease inhibitor (40 U/μL, code D2313A) were purchased from TaKaRa Biotechnology Co., Ltd., Dalian, China. Other chemicals were all purchased from Beijing Chemical Factory, Beijing, China. All chemicals mentioned above were used as received.

2.2. Preparation of CdTe-oligonucleotide conjugates

CdTe QDs stabilized by TGA were synthesized according to the method reported previously [34,35], and the as-prepared CdTe QDs with the emission wavelength at 610 nm was used in current investigations. All 5′ amine-terminated oligonucleotides used in this research were provided by Sangon Biological Engineering Technology and Services, Shanghai, China. The base sequence of oligonucleotides is shown below. The underlined nucleotides are phosphorothioate-modified. 5′ amine-terminated anti-survivin antisense oligonucleotides(ASON29): 5′-NH_2-AAA AAA AAA CCC AGC CTT CCA GCT CCT TG; survivin sense oligonucleotides(SON29): 5′-NH_2-AAA AAA AAA CAA GGA GCT GGA AGG CTG GG; A5: 5′-NH_2-AAA AA; A29: 5′-NH_2-AAA AAA AAA AAA AAA AAA AAA AAA AA; A40: 5′-NH_2-AAA AAA AAA AAA AAA AAA AAA AAA AAA AAA AAA A. For the preparation of CdTe-oligonucleotide conjugates, the CdTe QDs were activated in 1×PBS containing EDC and sulfo-NHS (CdTe QDs:EDC:sulfo-NHS = 1:1000:2500) for 15 min under gentle stirring. Then 5′ amine-terminated oligonucleotide was introduced (CdTe QDs:oligonucleotide = 1:25) under gentle mixing for 4 h in 1×PBS. The final CdTe-oligonucleotide conjugates were characterized using 3% agarose gel electrophoresis and then stored at 4 °C for 24 h before used.

For calculating the conjugation efficiency, the CdTe-ASON29 were purified by 10KD and 30KD centrifugal filters (Millipore) to remove the excess EDC/sulfo-NHS and ASON29, respectively. After the concentration of CdTe QDs were normalized, the absorbance at 260 nm of the purified CdTe-ASON29 by 10KD ($A_{260,A}$) and 30KD ($A_{260,B}$) centrifugal filter were measured, respectively. By a similar method, the absorbance at 260 nm of EDC/sulfo-NHS-activated CdTe QDs as a control was measured and denoted as $A_{260,C}$. The conjugation efficiency was defined as $(A_{260,B}-A_{260,C})/(A_{260,A}-A_{260,C})$.

2.3. Transfection of cells by CdTe-oligonucleotide conjugates

HeLa cells were obtained from the Cell Resource Center, IBMS, CAMS/PUMC, Beijing, China, and were cultured in EMEM supplemented with 10% (v/v) FBS at 37 °C in an atmosphere containing 5% CO_2. One day before transfection, HeLa cells were trypsinized with 0.25% (w/v) trypsin-0.53 mM EDTA solution and plated into 6-, 96-well cell culture plates, 96-well cell assay plates (Corning Incorporated) or glass-bottom tissue culture plates (MatTek) overnight to achieve 60–80% confluence. For transfection, cultured cells were firstly washed with 1×PBS and then incubated with CdTe QDs or CdTe-oligonucleotide conjugates for different periods of time at 37 °C in a CO_2 incubator.

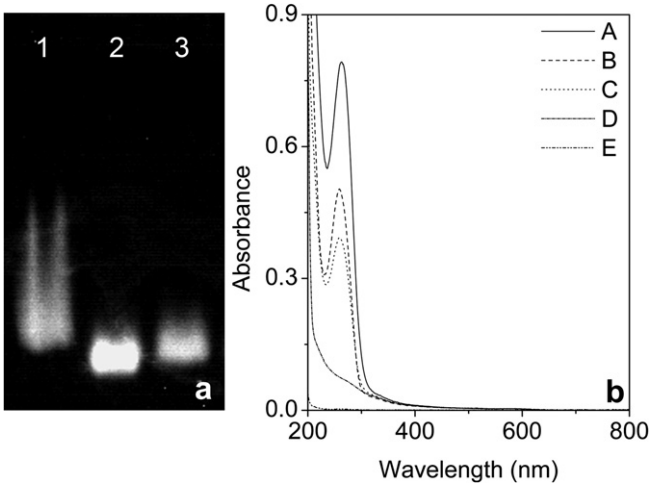

Fig. 1. Determination of the conjugate of CdTe QDs and ASON29. (a) 3% agarose gel electrophoresis of EDC/sulfo-NHS-activated CdTe QDs (Lane 1), CdTe QDs (Lane 2) and CdTe-ASON29 (Lane 3), the fluorescence image of the gel was captured under UV irradiation. (b) Absorption spectra of the CdTe-ASON29 before ultrafiltration (A), after ultrafiltration to remove unreacted EDC/sulfo-NHS (B) and ASON29 (C), EDC/sulfo-NHS-activated CdTe QDs after ultrafiltration (D) and the filtrate (E).

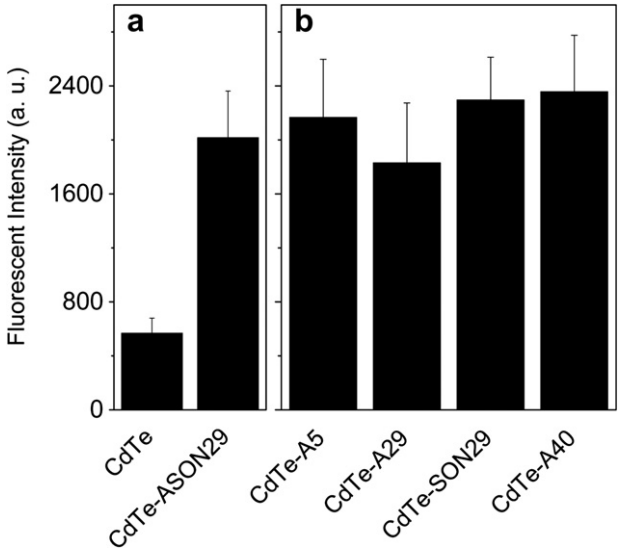

Fig. 2. Cellular uptake of CdTe QDs and CdTe-ASON29 (a), as well as other CdTe-oligonucleotide conjugates (b). All measurements were performed on one microplate, and the error bars represent means ± SD ($n = 3$).

2.4. Cellular uptake of CdTe-oligonucleotide conjugates

For quantitatively determining the cellular uptake of CdTe-oligonucleotide conjugates, HeLa cells were plated into 96-well cell assay plates and then transfected with CdTe QDs or CdTe-oligonucleotide conjugates for 60 min at 37 °C. After that, the transfected cells were washed twice with 1×PBS and subsequently subjected to fluorescence measurements by SpectraMax M5 microplate reader (Molecular Devices, Inc.). The excitation and emission detection wavelengths were set to 405 nm and 620 nm, respectively. To investigate the effects of temperature on the cellular uptake of CdTe-oligonucleotide conjugates, the HeLa cells were incubated with CdTe-oligonucleotide conjugates at 4 °C and 37 °C, for 30 min. The fluorescence imaging of the resultant cells was then performed on the FV 1000 confocal laser scanning microscope (OLYMPUS, Tokyo, Japan) using 488 nm laser excitation, and 100× objective (UPLSAPO/N.A. = 1.40). To study the effects of various endocytosis inhibition reagents on the uptake of CdTe-oligonucleotide conjugates, the HeLa cells were treated with chlorpromazine (20 μg/mL for 1 h), MβCD (16 mM for 35 min), genistein (100 μg/mL for 30 min), amiloride (2.5 mM for 35 min) and cyto D (6 μM for 30 min), following which the cells were washed with 1×PBS and incubated with CdTe-oligonucleotide conjugates for 30 min before fluorescence imaging.

2.5. Down-regulation of survivin mRNA by CdTe-ASON29

Real-time PCR was used to investigate the effect of CdTe-ASON29 on the down-regulation of survivin mRNA. Typically, the HeLa cells were firstly transfected for 1 h with CdTe QDs, CdTe-SON29 and CdTe-ASON29, respectively, and then cultured for 24 h at 37 °C. After that, the cells were harvested, and the total RNA was extracted from the cells using TRIzol reagent according to the manufacturer's protocol. The extracted RNA (1 μg) was then reverse transcribed to cDNA using reverse transcription reagents: dNTP (500 μM each), Oligo $d(T)_{18}$ (2.5 μM), M-MLV reverse transcriptase (200 U) and ribonuclease inhibitor (20 U). The transcribed cDNA was used as a template to amplify survivin cDNA using Taqman gene expression assays (Applied Biosystems, assay ID Hs00153353_mL) and Taqman universal PCR master mix (Applied Biosystems, part 4440049) on StepOnePlus real-time PCR system (Applied Biosystems). The relative quantification of survivin expression was performed using actin as an internal standard. Briefly, the amount of each survivin cDNA was normalized to that of actin cDNA and then compared with untreated cells to determine the expression level.

2.6. Measurement of cell viability

The colorimetric MTT assay was performed to determine the viability of HeLa cells. Briefly, HeLa cells were transfected for 1 h

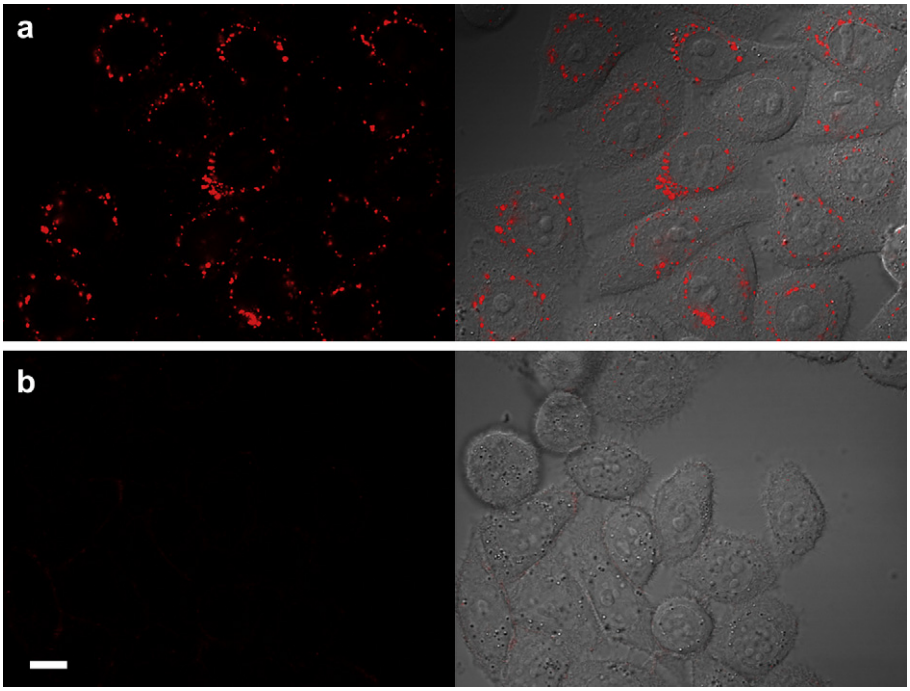

Fig. 3. Dark (left row) and merged field images (right row) of HeLa cells incubated with CdTe-ASON29 at 37 °C (a) and 4 °C (b), respectively. The scale bar in micrograph corresponds to 10 μm.

with CdTe QDs, CdTe-SON29 and CdTe-ASON29, respectively, and then cultured for 72 h at 37 °C. Subsequently, the cells were washed twice with 1×PBS, and 20 μL of MTT (5 mg/mL) were then added and allowed to react with the cells for 4 h before the addition of 150 μL DMSO for dissolution of the precipitation. Finally, the absorption of each solution was measured at 490 nm on SpectraMax M5 microplate reader.

2.7. Time-lapse fluorescence imaging of CdTe-oligonucleotide conjugates

For time-lapse fluorescence imaging, the HeLa cells were cultured in glass-bottom tissue culture plates. On the day of experiments, the cultured cells were incubated with CdTe-ASON29 or CdTe-SON29, for 20 min, 40 min and 60 min. At each given time point, one plate of cells was washed twice with 1×PBS, and then imaged on FV 1000 confocal laser scanning microscope using a 488 nm laser as excitation light source. At different time points, fresh cell samples were used to minimize the interference from previous measurements.

3. Results and discussion

3.1. Conjugate of CdTe QDs and ASON29

The absorption and fluorescence spectra of the as-prepared CdTe QDs used in the current investigations are presented in Supplemental Figure S1. The diameter of the CdTe QDs was estimated to be 3.5 nm, and the room temperature fluorescence quantum yield was estimated to be ~61% according to literature methods [36,37]. For preparing the mRNA probes, ASON29 (5′-NH_2-AAA AAA AAA CCC AGC CTT CCA GCT CCT TG, the underlined nucleotides are phosphorothioate-modified) were covalently conjugated with the carboxylate group of TGA on the surface of CdTe QDs, using EDC/sulfo-NHS-mediated amidation reaction. 3% agarose gel electrophoresis was used to evaluate the effectiveness

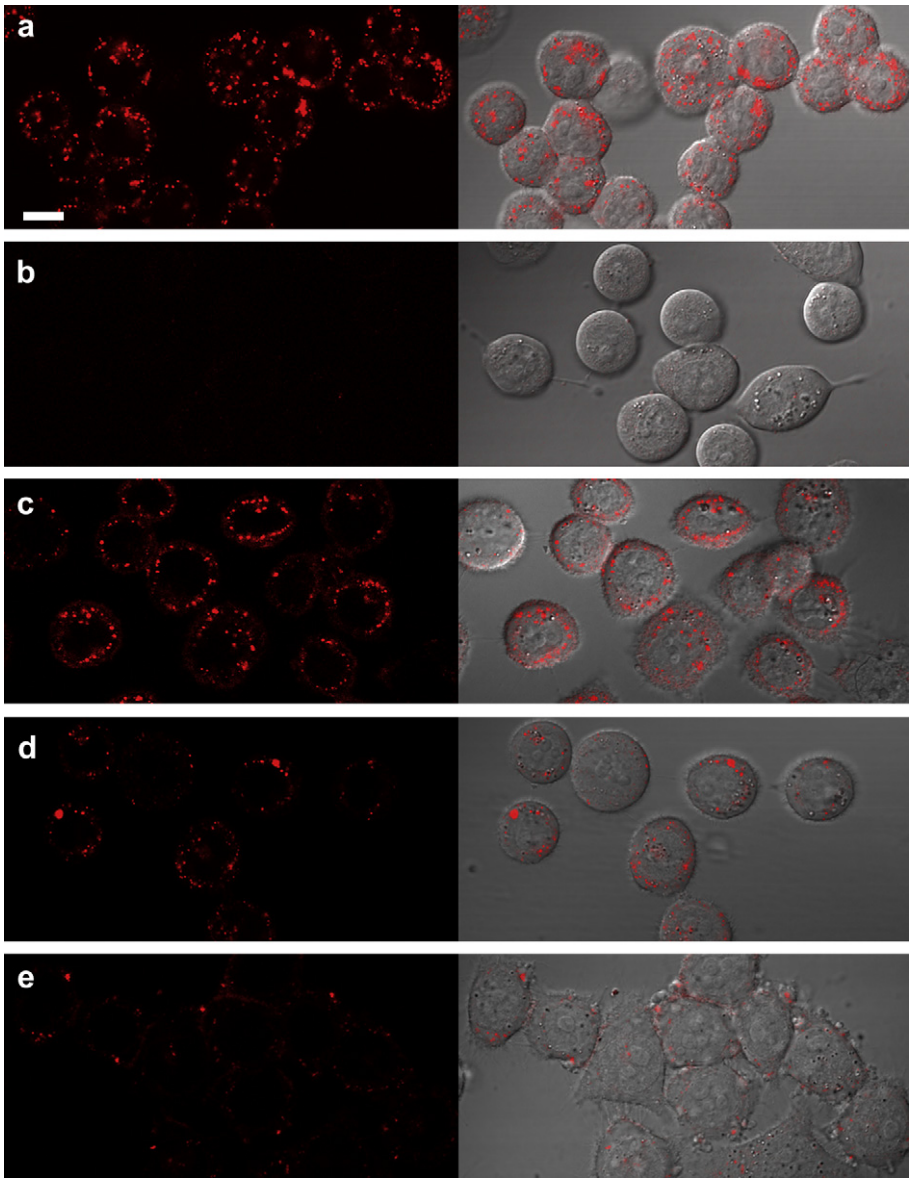

Fig. 4. Comparison of the cellular uptake of CdTe-ASON29 by HeLa cells treated with different types of endocytosis inhibition reagents: chlorpromazine (a), MβCD (b), genistein (c), amiloride (d) and cyto D (e). The scale bar in micrograph corresponds to 10 μm.

of the coupling reaction. A group of typical experimental results obtained under optimized conditions are shown in Fig. 1a. The EDC/sulfo-NHS-activated CdTe QDs (Lane 1) migrate obviously slower than the original CdTe QDs (Lane 2), which suggests that the CdTe QDs surface carboxylate groups were effectively activated by EDC and sulfo-NHS. Also, upon addition of amine-terminated ASON29, the mobility of activated CdTe QDs was increased but still slower than the original CdTe QDs (Lane 3) which implies that ASON29 was successfully coupled to CdTe QDs. Fig. 1b shows the absorption spectra of the EDC/sulfo-NHS-activated CdTe QDs and CdTe-ASON29 before and after ultrafiltration. Based on the change of absorbance at 260 nm, the conjugation efficiency of CdTe-ASON29 is calculated to be about 74%, and the number of ASON29 per CdTe QDs is about 18. These results further support the successful conjugation between CdTe QDs and ASON29. By a similar method, a conjugate of CdTe QDs and SON29 (5′-NH_2-AAA AAA AAA CAA GGA GCT GGA AGG CTG GG) was prepared as a control for CdTe-ASON29 and denoted as CdTe-SON29.

3.2. Cellular uptake and endocytic mechanism of CdTe-ASON29 conjugates

As an effective cellular uptake is of utmost importance for mRNA probes, fluorescence microplate reading method was used to evaluate the cellular uptake of the probes mentioned above by assuming that the fluorescence intensity of cells is proportional to the amount of the probes being uptaken. The results shown in Fig. 2a suggest that surface modification of oligonucleotides greatly increases the uptake of the CdTe-ASON29 by HeLa cells. To further illustrate the effects of the base sequence and length of oligonucleotides on the cellular uptake of the resultant probes, the following series of model probes, i.e., CdTe-A5, CdTe-A29, and CdTe-A40, were prepared accordingly and used together with CdTe-SON29 as controls for CdTe-ASON29. The results provided in Fig. 2b further reveal that the cellular uptake of the oligonucleotide-modified CdTe QDs is relatively independent of the base sequence and the length of oligonucleotides attached. On an average, the cellular uptake efficiency for CdTe-oligonucleotide conjugates is increased by a factor of four in comparison with the non-modified CdTe QDs. Positively charged gene vectors have widely been used in gene transfection. However, an effective cellular uptake of 13 nm negatively charged Au nanoparticles modified with ASON has also been observed [30,38–43]. Therefore, it is interesting to know the mechanism leading to the enhanced cellular uptake efficiencies of negatively charged nanoparticles modified by oligonucleotides.

To demonstrate the nature of the cellular uptake of the CdTe-oligonucleotides probes shown in Fig. 2, a set of comparable experiments were performed by incubating CdTe-ASON29 with HeLa cells at 4 °C and 37 °C, respectively. The results shown in Fig. 3 clearly reveal that the cellular uptake of CdTe-ASON29 is significantly decreased at 4 °C, which implies that cellular uptake of CdTe-ASON29 is through an energy-dependent endocytosis [17].

In general, the endocytosis of gene vectors may follow different endocytic pathways, e.g., clathrin-dependent endocytosis, caveolae-dependent endocytosis, macropinocytosis or other clathrin/caveolae-independent endocytosis [44]. Experimentally, the endocytic pathways are differentiated by using various types of inhibition agents, which were also adopted in the current investigations. In general, the HeLa cells largely change their shapes after being treated with chlorpromazine (Fig. 4a), MβCD (Fig. 4b), genistein (Fig. 4c), amiloride (Fig. 4d), and cyto D (Fig. 4e). Nonetheless, the variations in cellular uptake of the CdTe-ASON29 probes can be identified by confocal fluorescence microscope. It is quite obvious that chlorpromazine is hardly effective in suppressing the uptake of CdTe-ASON29, suggesting that clathrin-mediated endocytosis is

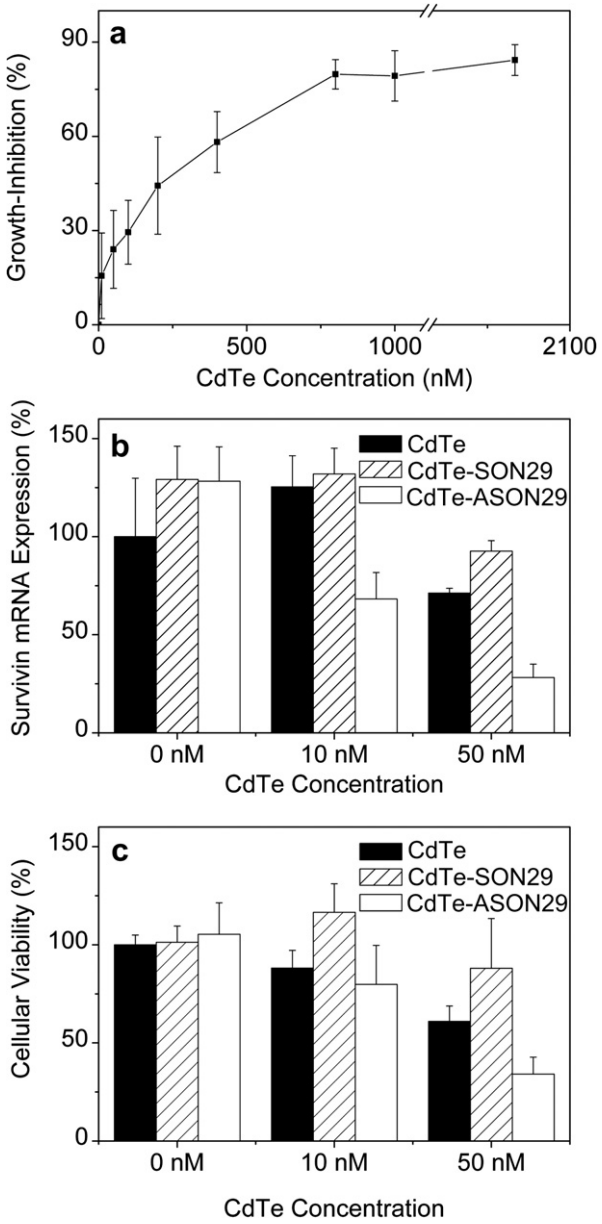

Fig. 5. The concentration-dependent growth-inhibition of HeLa cells by CdTe QDs (a), together with the effects of CdTe QDs, CdTe-SON29 and CdTe-ASON29 on the expression of survivin mRNA (b), and viability of HeLa cells (c) at given concentrations. Error bars represent means ± SD ($n = 3$).

not a dominant procedure involved, as chlorpromazine is known for suppressing clathrin-mediated endocytosis [45]. In contrast, the lipid rafts inhibition reagent MβCD can greatly inhibit the uptake of CdTe-ASON29, implying that the endocytosis of CdTe-ASON29 is lipid rafts-dependent [46]. Lipid rafts are the specialized membrane microdomains enriched in phospholipids, cholesterol, glycosphingolipids, and certain proteins [46], which are considered to be associated with caveolae-mediated endocytosis. Nevertheless, the results shown in Fig. 4c reveal that the endocytosis of CdTe-ASON29 can hardly be inhibited by genistein which is typically used for inhibiting the caveolae-mediated endocytosis [46], implying that the endocytosis of CdTe-ASON29 is through macropinocytosis that is recently demonstrated to involve lipid rafts as well [47]. The results shown in Fig. 4d and e obtained in the presence of amiloride and cyto D, respectively, obviously support the macropinocytosis mechanism. Further experiments based on CdTe-SON29, CdTe-A5,

CdTe-A29 and CdTe-A40 (Supplemental Figures S2–S9) suggest that macropincytosis is a general endocytic mechanism for the CdTe-oligonucleotide probes, relatively independent of the length and base sequence of the oligonucleotides modified on CdTe QDs.

As a matter of fact, the aforementioned endocytic mechanisms are more often used to interpret the cellular uptake of cationic gene vectors. However, the results shown in Fig. 4 and Supplemental Figures S2–S9 strongly support that the anionic CdTe-oligonucleotide conjugates also follow certain endocytic pathways, which may be because that the nanoscale protrusion and depressions of membrane with radii smaller than that of the nanoparticles are helpful for minimizing the repulsive interaction between negatively charged nanoparticles and cellular membrane, and enhancing the subsequent uptake of the anionic nanoprobes as well [44,48].

3.3. Down-regulation of survivin mRNA and apoptosis of HeLa cells induced by CdTe-ASON29

For an effective gene transfection, the transfected genes should be able to exert their biological functions after cellular uptake. Therefore, the effectiveness of CdTe-ASON29 on the down-regulation of survivin mRNA and apoptosis of HeLa cells were further investigated. As a gene transfection vector, CdTe QDs should exhibit as small as possible an impact on the cellular viability. Therefore, the effect of the concentration of CdTe QDs on cellular viability was firstly optimized using an MTT assay. As expected, the degree of cellular inhibition increases with the concentration of CdTe QDs, as shown in Fig. 5a. The IC_{50} (50% inhibitory concentration) value was estimated to be around 275.9 ± 61.0 nM by theoretically fitting the inhibition results. Then, two concentrations of CdTe QDs below the IC_{50} value, 10 nM and 50 nM at which the cellular viability remained at 84.4 ± 13.6% and 76.0 ± 12.3%, respectively, were chosen for further gene transfection experiments.

The effects of CdTe-ASON29 on the down-regulation of survivin mRNA were investigated using real-time PCR using CdTe QDs and CdTe-SON29 as negative controls. As shown in Fig. 5b, although 50 nM CdTe QDs inhibit the expression of survivin mRNA to some extent, the modification of nonfunctional SON29 on the surface of CdTe QDs can effectively suppress the inhibition effects of CdTe QDs on survivin mRNA expression with a relative survivin mRNA expression level reaching 92.6 ± 5.3%. In contrast, both 10 nM and 50 nM CdTe-ASON29 can effectively inhibit the expression of survivin mRNA. Especially, when the concentration of CdTe-ASON29 is 50 nM, the relative survivin mRNA expression level reaches 28.2 ± 6.8%, much lower than that from the control groups, which demonstrates that CdTe-ASON29 can specifically down-regulate the survivin mRNA expression.

Earlier investigations have demonstrated that the down-regulation of survivin mRNA by ASON can inhibit survivin translation, which then decreases the negative regulation of survivin to caspases-3 and -7 that act as common downstream parts of the two major apoptosis pathways, and consequently the apoptosis occurs [33]. To further reveal the overall effects of CdTe-ASON29 on apoptosis of HeLa cells, an MTT assay was performed again using CdTe QDs and CdTe-SON29 as negative controls. The results obtained are shown in Fig. 5c. Well in consistence with the mRNA expression experiments, the surface modification of SON29 can effectively decrease the cellular growth-inhibition of CdTe QDs, which makes the inhibition effects of CdTe-ASON probes at given probe concentrations even more pronounced. Therefore, it can be concluded that CdTe-ASON29 contributes largely to the inhibition of the cell viability by down-regulating survivin mRNA and consequently enhancing the apoptosis effects on HeLa cells. In addition, the results shown in Fig. 5b and c also suggest that oligonucleotides can generally be used as an inert material to suppress the cytotoxicity of QDs, which might pave a new route for further developing various QD-based probes for biology and biomedicine investigations.

3.4. Visually tracking the intracellular localization of CdTe-ASON29

On the basis of the aforementioned investigations on cellular uptake and biological functions of the CdTe-ASON29 probes, the intracellular localization of CdTe-ASON29 was visually tracked under a confocal fluorescence microscope so as to further correlate the biological functions of CdTe-ASON29 and its intracellular localization.

As CdTe-ASON29 can clearly induce the down-regulation of survivin mRNA and the following apoptosis of HeLa cells at 50 nM, in the following experiments the concentrations of both CdTe-ASON29 and its control CdTe-SON29 were set to 50 nM to obtain bright enough fluorescence image. Time-lapse imaging results presented in Fig. 6 reveal that within 20 min both CdTe-ASON29 and CdTe-SON29 are mainly found on both the plasma membrane and

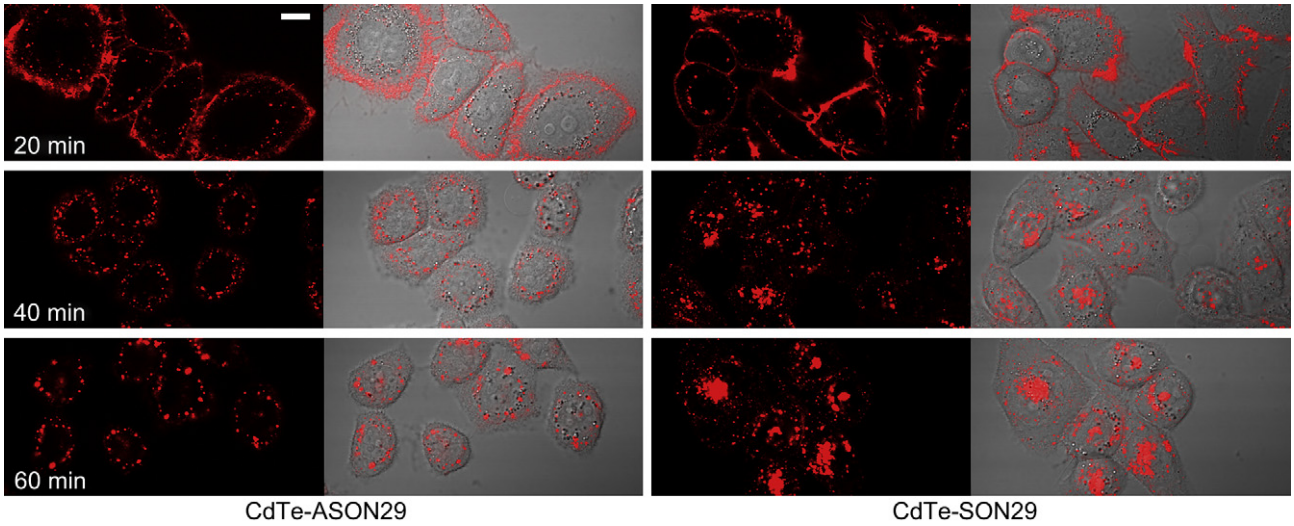

Fig. 6. Dark and merged field images of HeLa cells incubated with CdTe-ASON29 or CdTe-SON29 for different periods of time. The scale bar in micrograph corresponds to 10 μm.

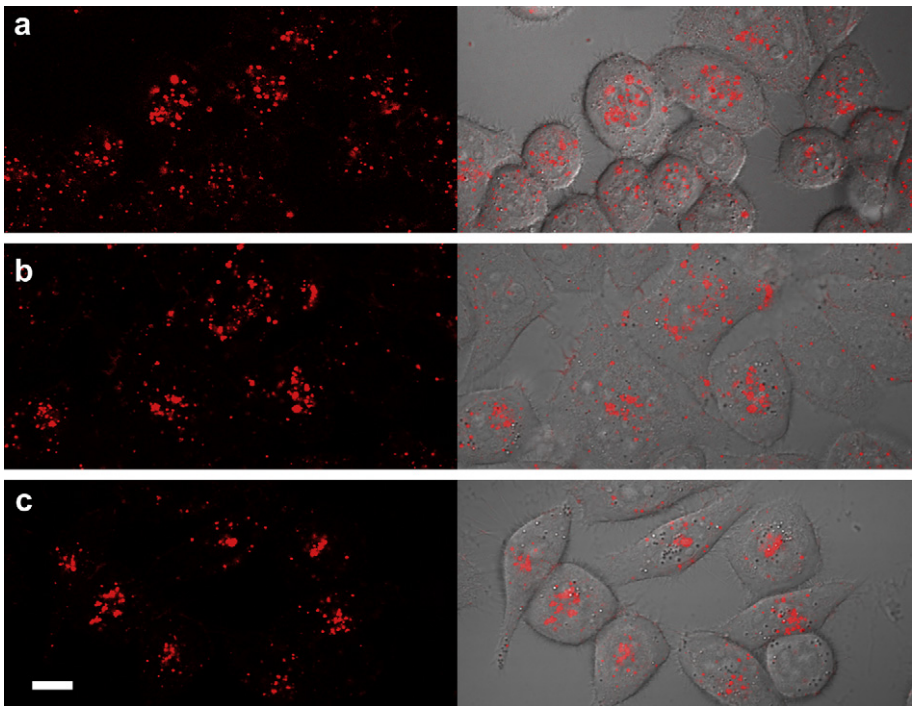

Fig. 7. Dark and merged field images of HeLa cells obtained after incubation for 60 min with CdTe-A5 (a), CdTe-A29 (b), and CdTe-A40 (c), respectively. The scale bar in micrograph corresponds to 10 μm.

filopodia. The latter is known to be involved in virus transport from infected cells to healthy ones [49,50]. Although it is still unclear whether filopodia is involved in nanoparticle endocytosis with respect to the current probes, the attachment of Tat peptide-conjugated QDs on filopodia was also observed while the intracellular uptake occurred [51]. Therefore, it can be speculated that the filopodia may also play a role in the endocytosis of QDs. In addition to the surface attachment, both CdTe-ASON29 and CdTe-SON29 also start to appear inside the cells at 20 min, mainly in the vicinity of the cell peripheries with a little amount of the probes being around the nucleus. No apparent difference in the intracellular locations is presented between CdTe-ASON29 and CdTe-SON29. However, differences in intracellular distribution of the probes start to appear at 40 min. With respect to CdTe-ASON29, the probes mainly localize in the cytoplasm but showing a tendency of being accumulated around the nucleus, which can better be seen at 60 min. In contrast, some of the CdTe-SON29 probes start to enter the nucleus at 40 min, and eventually most of the probes accumulate in the nucleolus at 60 min with the rest being arbitrarily distributed within the cells.

To further discover whether the distinct localization of CdTe-ASON29 is associated with the biological functions of ASON29, CdTe-A5, CdTe-A29 and CdTe-A40 were used as negative controls for revealing the probes distribution at 60 min. In general, as shown in Fig. 7, the intracellular distributions of the CdTe-A5, CdTe-A29 and CdTe-A40 follow the behavior of CdTe-SON29. Therefore, it is reasonable to conclude that the specific perinuclear localization of CdTe-ASON29 is directly correlated to the biological functions of ASON for survivin mRNA down-regulation and apoptosis induction.

The correlation between specific localization of anti-survivin ASON and its biological functions is essential for understanding the associated mechanisms. Down-regulation of survivin mRNA by anti-survivin ASON is mainly attributed to the activation of various mechanisms after its binding to survivin mRNA. The best understood mechanism is that endogenous RNase H recognizes and cleaves the mRNA/oligonucleotides duplex at the same location. As the RNase H is a family of enzymes expressed ubiquitously in cells, the cleavage of mRNA therefore may occur either in cytoplasm or in nucleus [52]. However, the current results on visually tracking the CdTe-ASON29 probes suggest that ASON quite probably takes effect in cytoplasm and in perinuclear regions, supported by the fact that the control probes can readily enter the nucleolus over the same period of time. A similar localization of siRNA in perinuclear region was also observed in RNAi (RNA-mediated interference), which was demonstrated to be associated with the gene down-regulation efficiency of siRNA [53]. In fact, both ASON and siRNA follow similar antisense mechanisms by inducing cleavage of target mRNA after specific binding [54]. Therefore, it can be deduced that the perinuclear region is the location where the antisense regulation process occurs. In addition, because the down-regulation of survivin mRNA by ASON29 ultimately leads to the apoptosis of HeLa cells, the accumulation of the CdTe-ASON29 probes in the perinuclear region - visualized through fluorescence - can specifically be correlated to the apoptosis of the HeLa cells, which may provide an alternative strategy for analyzing the early stages of apoptosis induced by survivin deficiency.

4. Conclusions

In summary, by covalently conjugating anti-survivin ASON to TGA-capped CdTe QDs, a fluorescent system for gene transfection and intracellular visualization of transfected genes has been achieved. Systematic investigations reveal that the cellular uptake of the negatively charged CdTe-oligonucleotide conjugates is through the macropinocytosis pathway. Further real-time PCR and MTT experimental results demonstrate that the ASON attached on the surface of the QDs can specifically induce the down-regulation of the survivin mRNA and ultimately induce the apoptosis of HeLa cells. Benefiting from the fluorescence of CdTe QDs, the visualization of the intracellular localization of the CdTe-ASON probes is consequently allowed. Systematic results suggest that the perinuclear region is the location where the antisense regulation process occurs. In addition, the current investigations also reveal that the surface

modification of oligonucleotide can effectively suppress the cytotoxicity of the CdTe QDs, which may expand the applications of QDs in cell biology investigations after further improvement. In conclusion, the current investigations reveal that CdTe QDs can not only be used as gene vectors but also offer the possibility of visually tracking the intracellular localization of a given oligonucleotide, thereby providing the possibilities to correlate the gene functions with their specific intracellular localization.

Acknowledgments

This work was financially supported by NSFC projects (20773140, 20820102035, 81090271) and National Basic Research Program of China (2011CB935800). The authors are grateful to Dr. D. Han from the National Center of Nanoscience and Nanotechnology, China, for his valuable suggestions with respect to confocal microscope measurements.

Appendix. Supplementary data

Methods for statistical analysis of results on cellular uptake of CdTe-oligonucleotide conjugates, regulation of survivin mRNA, and cell viability; Cellular uptake studies of CdTe-SON29, CdTe-A5, CdTe-A29 and CdTe-A40 by confocal microscopy. This material can be found in the on-line version, at doi:10.1016/j.biomaterials.2010.11.024.

References

[1] Alivisatos AP. Semiconductor clusters, nanocrystals, and quantum dots. Science 1996;271:933–7.
[2] Bruchez M, Moronne M, Gin P, Weiss S, Alivisatos AP. Semiconductor nanocrystals as fluorescent biological labels. Science 1998;281:2013–6.
[3] Chan WCW, Nie SM. Quantum dot bioconjugates for ultrasensitive nonisotopic detection. Science 1998;281:2016–8.
[4] Wang SP, Mamedova N, Kotov NA, Chen W, Studer J. Antigen/antibody immunocomplex from CdTe nanoparticle bioconjugates. Nano Lett 2002;2:817–22.
[5] Michalet X, Pinaud F, Bentolila LA, Tsay JM, Doose S, Li JJ, et al. Quantum qots for live cells, in vivo imaging, and diagnostics. Science 2005;37:538–44.
[6] Medintz IL, Uyeda HT, Goldman ER, Mattoussi H. Quantum dot bioconjugates for imaging, labeling and sensing. Nat Mater 2005;4:435–46.
[7] Hu FQ, Ran YL, Zhou ZA, Gao MY. Preparation of bioconjugates of CdTe nanocrystals for cancer marker detection. Nanotechnology 2006;17:2972–7.
[8] Somers RC, Bawendi MG, Nocera DG. CdSe nanocrystal based chem-/biosensors. Chem Soc Rev 2007;36:579–91.
[9] Gao XH, Yang LL, Petros JA, Marshal FF, Simons JW, Nie SM. In vivo molecular and cellular imaging with quantum dots. Curr Opin Biotech 2005;16:63–72.
[10] Pons T, Mattoussi H. Investigating biological processes at the single molecule level using luminescent quantum dots. Ann Biomed Eng 2009;37:1934–59.
[11] Chen AA, Derfus AM, Khetani SR, Bhatia SN. Quantum dots to monitor RNAi delivery and improve gene silencing. Nucleic Acids Res 2005;33:e190.
[12] Srinivasan C, Lee J, Papadimitrakopoulos F, Silbart LK, Zhao MH, Burgess DJ. Labeling and intracellular tracking of functionally active plasmid DNA with semiconductor quantum dots. Mol Ther 2006;14:192–201.
[13] Derfus AM, Chen AA, Min DH, Ruoslahti E, Bhatia SN. Targeted quantum dot conjugates for siRNA delivery. Bioconjug Chem 2007;17:1391–6.
[14] Tan WB, Jiang S, Zhang Y. Quantum-dot based nanoparticles for targeted silencing of HER2/neu gene via RNA interference. Biomaterials 2007;28:1565–71.
[15] Li D, Li G, Guo W, Li P, Wang E, Wang J. Glutathione-mediated release of functional plasmid DNA from positively charged quantum dots. Biomaterials 2008;29:2776–82.
[16] Qi L, Gao X. Quantum dot-amphipol nanocomplex for intracellular delivery and real-time imaging of siRNA. ACS Nano 2008;2:1403–10.
[17] Walther C, Meyer K, Rennert R, Neundorf I. Quantum dot-carrier peptide conjugates suitable for imaging and delivery application. Bioconjug Chem 2008;19:2346–56.
[18] Yezhelyev MV, Qi L, O'Regan RM, Nie S, Gao X. Proton-sponge coated quantum dots for siRNA delivery and intracellular imaging. J Am Chem Soc 2008;130:9006–12.
[19] Jung JJ, Solanki A, Memoli KA, Kamei K, Kim H, Drahl MA, et al. Selective inhibition of human brain tumor cells through multifunctional quantum-dot-based siRNA delivery. Angew Chem Int Ed 2010;49:103–7.
[20] Lee H, Kim IK, Park TG. Intracellular trafficking and unpacking of siRNA/quantum dot-PEI complexes modified with and without cell penetrating peptide: confocal and flow cytometric FRET analysis. Bioconjug Chem 2010;21:289–95.
[21] Ho YP, Chen HH, Leong KW, Wang TH. Evaluating the intracellular stability and unpacking of DNA nanocomplexes by quantum dots-FRET. J Control Release 2006;116:83–9.
[22] Li PC, Li D, Zhang LX, Li GP, Wang EK. Cationic lipid bilayer coated gold nanoparticles-mediated transfection of mammalian cells. Biomaterials 2008;29:3617–24.
[23] Liu JW, Stace-Naughton A, Brinker CJ. Silica nanoparticle supported lipid bilayers for gene delivery. Chem Commun 2009;34:5100–2.
[24] Zhou XF, Zhang XH, Yu XH, Zha X, Fu Q, Liu B, et al. The effect of conjugation to gold nanoparticles on the ability of low molecular weight chitosan to transfer DNA vaccine. Biomaterials 2008;29:111–7.
[25] Song WJ, Du JZ, Sun TM, Zhang PZ, Wang J. Gold nanoparticles capped with polyethyleneimine for enhanced siRNA delivery. Small 2010;6:239–46.
[26] Xia TA, Kovochich M, Liong M, Meng H, Kabehie S, George S, et al. Polyethyleneimine coating enhances the cellular uptake of mesoporous silica nanoparticles and allows aafe delivery of siRNA and dNA constructs. ACS Nano 2009;3:3273–86.
[27] Jia NQ, Lian Q, Shen HB, Wang C, Li XY, Yang ZN. Intracellular delivery of quantum dots tagged antisense oligodeoxynucleotides by functionalized multiwalled carbon nanotubes. Nano Lett 2007;7:2976–80.
[28] Arsianti M, Lim M, Marquis CP, Amal R. Assembly of polyethylenimine-based magnetic iron oxide vectors: insights into gene delivery. Langmuir 2010;26:7314–26.
[29] Gonzalez B, Colilla M, de Laorden CL, Vallet-Regi M. A novel synthetic strategy for covalently bonding dendrimers to ordered mesoporous silica: potential drug delivery applications. J Mater Chem 2009;19:9012–24.
[30] Rosi NL, Giljohann DA, Thaxton CS, Lytton-Jean Abigail KR, Han MS, Mirkin CA. Oligonucleotide-modified gold nanoparticles for intracellular gene regulation. Science 2006;312:1027–30.
[31] Mintzer MA, Simanek EE. Nonviral vectors for gene delivery. Chem Rev 2009;109:259–302.
[32] Ryan BM, O'Donovan N, Duffy MJ. Survivin: a new target for anti-cancer therapy. Cancer Treat Rev 2009;35:553–62.
[33] Olie AR, Simões-Wüst P, Baumann B, Leech SH, Fabbro D, Stahel RA, et al. A novel antisense oligonucleotide targeting survivin expression induces apoptosis and sensitizes lung cancer cells to chemotherapy. Cancer Res 2000;60:2805–9.
[34] Gaponik N, Talapin DV, Rogach AL, Hoppe K, Shevchenko EV, Kornowski A, et al. Thiol-capping of CdTe nanocrystals: an alternative to organometallic synthetic routes. J Phys Chem B 2002;106:7177–85.
[35] Rogach AL, Franzl T, Klar TA, Feldmann J, Gaponik N, Lesnyak V, et al. Aqueous synthesis of thiol-capped CdTe nanocrystals: state-of-the-art. J Phys Chem C 2007;111:14628–37.
[36] Yu WW, Qu LH, Guo WZ, Peng XG. Experimental determination of the extinction coefficient of CdTe, CdSe, and CdS nanocrystals. Chem Mater 2003;15:2854–60.
[37] Bao HB, Gong YJ, Li Z, Gao MY. Enhancement effect of illumination on the photoluminescence of water-soluble CdTe nanocrystals: toward highly fluorescent CdTe/CdS core-shell structure. Chem Mater 2004;16:3853–9.
[38] Seferos DS, Giljohann DA, Hill HD, Prigodich AE, Mirkin CA. Nano-flares: probes for transfection and mRNA detection in living cells. J Am Chem Soc 2007;129:15477–9.
[39] Prigodich AE, Seferos DS, Massich MD, Giljohann DA, Lane BC, Mirkin CA. Nano-flares for mRNA regulation and detection. ACS Nano 2009;3:2147–52.
[40] Giljohann DA, Seferos DS, Prigodich AE, Patel PC, Mirkin CA. Gene regulation with polyvalent siRNA-nanoparticle conjugates. J Am Chem Soc 2009;131:2072–3.
[41] Zheng D, Seferos DS, Giljohann DA, Patel PC, Mirkin CA. Aptamer nano-flares for molecular detection in living cells. Nano Lett 2009;9:3258–61.
[42] Dhar S, Daniel WL, Giljohann DA, Mirkin CA, Lippard SJ. Polyvalent qligonucleotide gold nanoparticle conjugates as delivery vehicles for platinum (IV) warheads. J Am Chem Soc 2009;131:14652–3.
[43] Song Y, Xu X, MacRenaris KW, Zhang XQ, Mirkin CA, Meade T. Multimodal gadolinium-enriched DNA-gold nanoparticle conjugates for cellular imaging. Angew Chem Int Ed 2009;48:9143–7.
[44] Nel AE, Madler L, Velegol D, Xia T, Hoek EMV, Somasundaran P, et al. Understanding biophysicochemical interactions at the nano-bio intherface. Nat Mater 2009;8:543–57.
[45] Wang LH, Rothberg KG, Anderson RG. Mis-assembly of clathrin lattices on endosomes reveals a regulatory switch for coated pit formation. J Cell Biol 1993;123:1107–17.
[46] Vercauteren D, Vandenbroucke RE, Jones AT, Rejman J, Demeester J, De Smedt SC, et al. The use of inhibitors to study endocytic pathways of gene carriers: optimization and pitfalls. Mol Ther 2010;18:561–9.
[47] Chen B, Liu QL, Zhang YL, Xu L, Fang XH. Transmembrane delivery of the cell-penetrating peptide conjugated semiconductor quantum dots. Langmuir 2008;24:11866–71.
[48] Hoek EM, Agarwal GK. Extended DLVO interactions between spherical particles and rough surfaces. J Colloid Interface Sci 2006;298:50–8.
[49] Sherer NM, Lehmann MJ, Jimenez-Soto LF, Horensavitz C, Pypaert M, Mothes W. Retroviruses can establish filopodial bridges for efficient cell-to-cell transmission. Nat Cell Biol 2007;9:310–5.

[50] Lehmann MJ, Sherer NM, Marks CB, Pypaert M, Mothes W. Actin- and myosin-driven movement of viruses along filopodia precedes their entry into cells. J Cell Biol 2005;170:317–25.
[51] Ruan G, Agrawal A, Marcus AI, Nie S. Imaging and tracking of tat peptide-conjugated quantum dots in living cells: new insights into nanoparticle uptake, intracellular transport, and vesicle shedding. J Am Chem Soc 2007; 129:14759–66.
[52] Dean NM, Bennet CF. Antisense oligonucleotide-based therapeutics for cancer. Oncogene 2003;22:9087–96.
[53] Chiu YL, Ali A, Chu CY, Cao H, Rana TM. Visualizing a correlation between siRNA localization, cellular uptake, and RNAi in living cells. Chem Biol 2004;11:1165–75.
[54] Bennett CF, Swayze EE. RNA targeting therapeutics: molecular mechanisms of antisense oligonucleotides as a therapeutic platform. Annu Rev Pharmacol 2010;50:259–93.